electricity

MDPI

Article

Optimization-Based Residential PV Inverter Control for Reactive Power Support and Efficient Operation in Low-Voltage Networks

Angamuthu Ananth *, Sundaram Maruthachalam, Anand Mouttouvelou and Sivakumar Palaniswamy

Department of Electrical and Electronics Engineering, PSG College of Technology, Coimbatore 641004, Tamil Nadu, India; msm.eee@psgtech.ac.in (S.M.); and.eee@psgtech.ac.in (A.M.); psk.eee@psgtech.ac.in (S.P.)

* Correspondence: aam.eee@psgtech.ac.in

Abstract

The adoption of solar photovoltaic (PV) inverters in residential networks has increased significantly because of the growing demand for clean energy and carbon footprint reduction. While these systems enable utilities to reduce dependence on conventional energy sources, several operational challenges remain unaddressed at the prosumer level, including power factor (PF) penalties, voltage fluctuations, and underutilization of inverter capacity. Most commercially available residential inverters primarily focus on real power export and do not actively manage reactive power, leading to power quality issues in low-voltage distribution networks. In addition, emerging time-of-day (ToD) tariff structures are not effectively utilized by existing control strategies. In this work, an optimization-based supervisory control strategy is proposed for residential PV inverters. The problem is formulated as a convex quadratic programming (CQP) problem, where real and reactive power are optimally coordinated under inverter kilovolt-ampere constraints. The objective is to integrate ToD-based economic optimization with power factor regulation. Unlike conventional approaches that enforce strict PF constraints, the proposed method incorporates PF through a quadratic penalty on the deviation from the desired active–reactive power relationship, enabling a controlled trade-off between economic benefit and grid-support requirements. Depending on operating conditions, the controller dynamically prioritizes real power export or reactive power support while maintaining PF close to the desired threshold. Experimental validation is carried out on a 6 kVA hardware prototype. The results demonstrate improved inverter utilization, enhanced power factor performance, and significant cost reduction under the considered operating scenario. These findings highlight the potential of coordinated real and reactive power management for improving both economic and grid performance in residential PV systems.

Keywords: solar photovoltaic system; inverter optimization; power factor regulation; real power export; economic dispatch; time-of-day tariff

Check for updates

Academic Editor: Angel Arcos-Vargas

Received: 4 March 2026
Revised: 29 April 2026
Accepted: 1 May 2026
Published: 31 May 2026

Copyright: © 2026 by the authors. Licensee MDPI, Basel, Switzerland. This article is an open access article distributed under the terms and conditions of the Creative Commons Attribution (CC BY) license.

1. Introduction

The rapid increase in residential solar photovoltaic (PV) systems in low-voltage (LV) distribution networks is transforming the operation of power grids. PV systems provide environmental and economic benefits; as power is generated locally, dependence on centralized plants is reduced, and excess energy can be exported to the grid [1,2]. However, this transition also introduces several operational challenges. When PV generation is high and local demand is low, reverse power flow can occur. This may cause voltage rise beyond

the allowed limit and voltage imbalance in single-phase and multi-phase feeders. Most of the installed residential inverters operate close to unity power factor and mainly focus on exporting real power. These inverters do not actively provide reactive power support at the PCC. As a result, voltage rise becomes more severe, feeder losses increase, and consumers may face penalties from utilities [3,4].

Solar power generation is also intermittent and varies with time. The net power exchanged between the household and the grid depends on both the load demand and available PV power. Since both are changing continuously, the operating condition of the system also changes frequently [5–11]. These variations can reduce power quality and may not use the inverter capacity effectively. In many conventional control methods, all available real power is exported to the grid without reactive power management. This approach does not properly address voltage limits or the economic performance of the installed system.

To address the above mentioned issues, research is moving towards optimization-based control methods. Multiple objectives such maintaining the voltage at the regulatory limit, reducing power losses, utilizing inverter capacity, and reducing voltage fluctuations can be handled by formulating the problem as a multi-period optimal power flow (OPF). Models such as LinDistFlow are widely used to represent the LV network. Such models can capture the influence of real and reactive power on voltage fluctuations [12–18]. Reports [19–24] have presented several advanced methods that demonstrably improve voltage regulation and loss reduction compared to conventional methods. Optimization-based approaches have also been applied at the transmission level for multi-objective optimal power flow incorporating FACTS devices [25,26], though such methods are designed for network-level dispatch rather than real-time embedded residential control.

Another important issue in residential systems is the shift from kilowatt (kW)-based billing to kilovolt-ampere (kVA)-based billing. In kW-based billing, only real power consumption is considered, whereas in a kVA-based billing, apparent power is considered. Furthermore, a low power factor leads to a penalty even if real energy use is the same. Many residential consumers are not fully aware of this change. If the inverter cannot provide reactive power support or manage apparent power properly, the household may face higher electricity bills. Therefore, inverter control strategies must consider both technical and economic aspects, especially under time-of-day (ToD) tariffs.

Motivated by these objectives, this paper focuses on an optimization-based control strategy for residential PV inverters in LV networks. A multi-period OPF problem is formulated to decide the optimal real and reactive power schedule of the inverter. The inverter rating, ToD tariffs, and voltage constraints are clearly included in the formulation. The method can be applied to single-phase as well as multi-phase feeders. The aim is to improve voltage quality, enhance inverter utilization, and enable coordinated techno-economic operation in residential systems.

The proposed method is formulated as a convex quadratic programming (CQP) problem, where the PF is incorporated through a quadratic penalty on the deviation from the desired active–reactive power relationship. This formulation enables a controlled trade-off between economic objectives and grid-support requirements, allowing the inverter to dynamically balance real and reactive power under varying operating conditions while ensuring convergence to a globally optimal solution due to convexity and computational efficiency.

Conventional Volt-VAR droop control strategies rely on predefined static characteristics and do not explicitly account for economic objectives or optimal allocation of inverter capacity. In contrast, the proposed optimization-based approach dynamically coordinates

real and reactive power by considering time-of-day tariffs, inverter constraints, and power factor requirements, enabling a techno-economic optimal operation.

The main contributions of this paper can be summarized as follows:

1. A supervisory control strategy is developed to manage the coordinated export of real and reactive power by the inverter without violating the power factor constraints or the inverter rating.
2. The optimized set points are derived using convex quadratic programming constraints and implemented on a laboratory prototype without modifying its internal control architecture.
3. Experimental validation on the hardware prototype demonstrates improved PF compliance, improved utilization of inverter capacity for real and reactive power export, and measurable economic benefit under ToD tariffs.

The remainder of the paper is organized as follows: Section 2 describes the system and explains the problem formulation. Section 3 presents the optimization method, including objective functions and constraints. Section 4 discusses the experimental results. Section 5 concludes the paper and discusses possible future work in optimization-based residential PV inverter control under ToD pricing and reactive power support.

2. System Description and Problem Formulation

The residential system under consideration in this study is explained in this section. The formulation includes the load, PV generation, and constraints influencing the real and reactive operation. It also includes the time-of-day operation and regulatory power factor penalty factors.

2.1. Household Power Balance

Consider a residential household connected to a radial LV distribution feeder. The household is also equipped with a rooftop photovoltaic (PV) system interfaced with the LV grid via an inverter. Let $P_{load}(t)$ and $Q_{load}(t)$ denote the real and reactive power demand of the household at time t, and let $P_{PV}(t)$ denote the instantaneous PV power generation. The inverter injects $P_{inv}(t)$ and $Q_{inv}(t)$, subject to its rated apparent power S_{inv}. The net real power exchanged with the grid is given by

$$P_{grid}(t) = P_{load}(t) - P_{PV}(t) - P_{inv}(t). \tag{1}$$

A similar expression holds for reactive power:

$$Q_{grid}(t) = Q_{load}(t) - Q_{inv}(t). \tag{2}$$

The imported and exported real power components are defined as follows:

$$P_{import}(t) = \max(P_{grid}(t), 0), \quad P_{export}(t) = \max(-P_{grid}(t), 0). \tag{3}$$

The household PCC power factor, which determines billing under emerging kVA-based tariffs, is defined as the ratio of real power to apparent power. Owing to its nonlinear nature, this expression is not directly incorporated into the optimization. Instead, an equivalent linear relationship between active and reactive power is adopted for the proposed formulation.

The desired power factor condition can be equivalently expressed as a linear relationship between active and reactive power, given by $Q_{grid}(t) = k\,P_{grid}(t)$, where $k = \tan(\cos^{-1}(PF_{target}))$. This relationship is used in the optimization formulation to

avoid the nonlinearity of the conventional power factor expression while preserving its physical meaning.

2.2. Inverter Capability and Constraints

Each PV inverter is constrained by its rated apparent power S_{inv}, which defines the feasible operating region:

$$P_{inv}^2(t) + Q_{inv}^2(t) \leq S_{inv}^2, \quad \forall t. \tag{4}$$

This enforces both thermal and electrical limits and couples real and reactive power output. Real power injection is further bounded by the available PV generation:

$$0 \leq P_{inv}(t) \leq P_{PV}(t), \quad \forall t, \tag{5}$$

ensuring that the inverter does not export more than the generated PV power. The reactive power can be allocated to maintain the PCC PF constraint while respecting the inverter's apparent power limit.

2.3. Time-of-Day Tariff Considerations

In contrast to a conventional tariff system, the price of electricity varies at different times of the day in a ToD tariff system. Let $C_{buy}(t)$ and $C_{sell}(t)$ denote the import and export prices at time t. The household inverter must operate to maximize economic benefit. The inverter cannot operate by importing real power while ignoring reactive power, as this would result in a power factor penalty. Focusing solely on improving the power factor ignores export revenue. Thus, the inverter requires an optimal operating mode that differs from that of conventional residential PV inverters.

2.4. Motivation for Optimization

The load connected, the PV generation and the ToD tariff change throughout the day. The inverter must control its real and reactive power export according to this for every change. Such an operating point cannot be determined using simple rule-based control as in a conventional system. Hence, such a commercially available inverter cannot be operated to ensure both technical and economic benefit. Furthermore, in most commercial inverters, the operating mode is set to export only real power even when PV generation is absent or reduced. The kVA capacity of the inverter remains underutilized. The proposed system attempts to utilized the remaining available capacity of inverter, thereby increasing the economic benefit of the installed system.

The proposed system utilizes an optimization strategy that provides a systematic way to determine the appropriate operating point for the inverter under the varying conditions described above. The optimization techniques ensure that the inverter obeys the regulatory norms and achieves economic benefits without violating its power rating. The optimization method is executed and implemented as a supervisory control in such a way as to decide the actual real and reactive power to be exported. This ensures that the inverter's internal control architecture is not modified and that its control performance remains unmodified. The proposed system works as a supervisory control and sends the required real and reactive power as a set reference command to the inverter.

Contributions of the Work: The main contributions of this paper to the field are as follows:

(1) A supervisory control strategy is developed to manage the export of real and reactive power by an inverter without violating the pf and inverter rating is developed.
(2) The optimized set points are derived using the constraints and implemented on a laboratory prototype without violating or changing its internal control architecture.

(3) Experimentation on the hardware prototype is performed to show improved PF compliance and better utilization of the inverter to manage real and reactive power export for economic benefit and power quality improvement.

3. Optimization-Based Inverter Control

This section explains the optimization framework developed for residential PV inverter control. The main objective is to reduce electricity cost and maximize economic benefit from export while maintaining the power factor close to the desired threshold under ToD tariffs. The framework combines an optimization problem with a supervisory control logic that can be implemented in real time. To clearly define the optimization problem, the decision variables and required notation for modeling inverter operation are introduced first.

At each discrete time step $t = 1, \ldots, T$, the inverter injects real power $P_{inv}(t)$ and reactive power $Q_{inv}(t)$, subject to its apparent power limit S_{inv}. The net power exchange with the grid at the PCC is given by (1) and (2), and the corresponding PCC power factor is defined as discussed in Section 2.1. These definitions establish the decision space of inverter set points and form the foundation for the optimization model. Building on this notation, the optimization problem is now formulated.

3.1. Optimization Problem Formulation

The multi-period optimization problem is formulated to minimize the total electricity cost over the horizon T while respecting inverter and PCC constraints:

$$\min_{P_{inv}(t), Q_{inv}(t)} \sum_{t=1}^{T} \Big[C_{buy}(t) P_{import}(t) - C_{sell}(t) P_{export}(t) \Big], \tag{6}$$

where $C_{buy}(t)$ and $C_{sell}(t)$ are the ToD-based import and export tariffs. Minimizing this cost inherently promotes real power export during high-tariff periods while reducing household import expenses.

To incorporate power factor regulation, a penalty-based formulation is introduced in the objective function. A quadratic penalty term is used to penalize deviations from the desired active–reactive power relationship.

The target power factor is fixed at $PF_{\text{target}} = 0.95$, and the weighting parameter is selected as $\lambda = 0.8$. These parameters are predefined and remain constant throughout the study. The adaptability of the controller arises from the repeated solution of the optimization problem under varying operating conditions, rather than any change in these parameters.

$$P_{inv}^2(t) + Q_{inv}^2(t) \leq S_{inv}^2, \tag{7}$$

$$0 \leq P_{inv}(t) \leq P_{PV}(t), \tag{8}$$

The optimization is subject to inverter apparent power limits, real power bounds, and reactive power feasibility constraints. Power factor regulation is handled through a penalty-based formulation within the objective function rather than as a strict constraint. Although the optimization framework provides the theoretical formulation, a supervisory control strategy is required to implement the framework in real time. Power factor regulation is incorporated by enforcing a quadratic penalty on the deviation from the desired linear relationship between active and reactive power, ensuring that the formulation remains a convex quadratic program. This enables a flexible trade-off between economic objectives and power factor performance, while preserving the convex quadratic structure of the optimization problem. The resulting optimization problem is a convex quadratic programming (QP) problem. The objective function consists of a linear economic term and a quadratic

penalty term for power factor regulation. All constraints, including the inverter's apparent power limits and operational bounds, define a convex feasible region.

Owing to the convexity of the region, there is a unique global optimum, and the optimization problem can be solved efficiently using standard QP solvers, ensuring reliable real-time implementation.

3.2. Supervisory Control Logic

The optimization framework is programmed as a hierarchical supervisory control procedure to deploy it in a real-time environment. At each time step, the following actions are performed:

1. Allocate reactive power $Q_{inv}(t)$ based on the optimization objective to improve power factor while respecting inverter constraints.
2. Assign the remaining inverter capacity to real power $P_{inv}(t)$ for economic dispatch based on ToD tariffs.
3. Continuously ensure that the apparent power limit of the inverter is not exceeded.
4. Update the inverter set points dynamically using measured PV generation and household load.

This enables implementation of the optimization framework on the existing inverter. Standard quadratic programming solvers such as the active set method and interior-point methods are utilized to solve the optimization in the controller. Interior-point methods are employed owing to their superior convergence properties and robustness for convex optimization problems.

4. Experimental Setup and Control Implementation

4.1. Hardware Configuration and Experimentation

To evaluate the proposed supervisory optimization control strategy, an experimental prototype is designed to emulate realistic residential load conditions using passive components. The key components are listed in Table 1. A schematic of the setup is shown in Figure 1.

Table 1. Laboratory prototype components.

Component	Specification
PV Emulator	0–400 V, 0–20 A
6 kVA Inverter	230 V AC, H-bridge, LCL filter
Resistive Load	0.5–4 kW selectable
Inductive Load	10–30 mH iron core
Voltage Sensor	Isolated, ±400 V
Current Sensor	Hall effect, ±30 A
DSP Controller	TI C2000, 150 MHz
Protection	Fuses, MCBs, isolation TX

The experimental test bed consists of a programmable DC supply that emulates PV generation. A grid-connected single-phase inverter, rated at 6 kVA, receives high-level P_{inv} and Q_{inv} set points from the supervisory controller while its internal voltage and current loops remain unchanged. Household loads are emulated using a mixture of resistive components (lamps, heaters) and inductive components (fans, motors) to replicate realistic residential demand profiles.

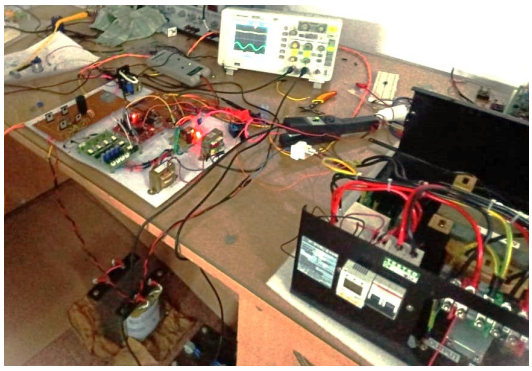


Figure 1. Residential PV test bed for supervisory optimization evaluation.

PCC voltage and current are continuously measured using calibrated voltage and current sensors, enabling real-time monitoring and feedback for the supervisory controller.

To evaluate the system, two operational scenarios were performed during experimentation: (i) the Base Case and (ii) Optimized Control. The characteristics of these scenarios were as follows:

1. Base Case: This depicts the case of a commercially available solar PV inverter. In this case, the inverter is programmed to export the real power to the grid without providing any reactive power support.
2. Optimized Control: In this case, the supervisory control algorithm is active. The supervisory control algorithm actively computes and commands the set points P_{inv} and Q_{inv} at each control interval. This enables us to evaluate the performance of the proposed strategy on the developed prototype.

To emulate realistic economic incentives, a time-of-day (ToD) tariff scheme is employed. The tariff values for each interval are summarized in Table 2.

Table 2. Hourly ToD tariff (Rs./kVAh)—folded column format.

Hour	Tariff	Hour	Tariff	Hour	Tariff
0	6.00	8	7.50	16	8.00
1	6.00	9	8.00	17	7.50
2	6.00	10	8.50	18	7.00
3	6.00	11	9.00	19	6.80
4	6.00	12	9.50	20	6.50
5	6.00	13	9.50	21	6.30
6	6.50	14	9.00	22	6.20
7	7.00	15	8.50	23	6.00

The experimental design ensures that all hardware, measurement, and tariff inputs are synchronized with the supervisory controller for real-time evaluation. The hourly load demand and PV generation profiles used in the experiments are explicitly provided in Table 3. The experimental conditions, including load variations and PV generation, are designed to reflect realistic residential operating scenarios over a 24-h cycle.

4.2. Controller Implementation

The proposed supervisory optimization control strategy is coded as a higher-level set point controller. The control strategy computes the optimal real (P_{inv}) and reactive (Q_{inv}) power commands and dispatches them as reference set points. This methodology ensures that the inner current loop and outer voltage control loop remain unaffected. The parameters for the reference set points are obtained from the higher-level supervisory control algorithm as mentioned previously. Such an implementation enables the control

algorithms of existing inverters to be upgraded easily without modifying the existing core control loops.

$$\min_{P_{\text{inv}},Q_{\text{inv}}} \quad \underbrace{C_{\text{buy}}P_{\text{import}} - C_{\text{sell}}P_{\text{export}}}_{\text{Economic Objective}} + \lambda \cdot \underbrace{\left(Q_{\text{grid}} - k\,P_{\text{grid}}\right)^2}_{\text{Power Factor Penalty}} \tag{9}$$

$$\text{subject to} \quad ...P_{\text{inv}}^2 + Q_{\text{inv}}^2 \leq S_{\text{inv}}^2 \tag{10}$$

$$0 \leq P_{\text{inv}} \leq P_{\text{PV}} \tag{11}$$

where $k = \tan\left(\cos^{-1}(\text{PF}_{\text{target}})\right)$ represents the desired power factor slope.

Table 3. Hourly PV output, load, grid, inverter compensation, cost (in Rs.), and savings with power factors.

Hour	PV (kW)	Before Optimization				After Optimization				
		Load $P + jQ$ (kVA)	Grid $P + jQ$ (kVA)	PF	Cost	Grid $P + jQ$ (kVA)	PF	Q_{inv}	Cost	Savings
0	0.00	$1.70 + j1.00$ (1.97)	$1.70 + j1.00$ (1.97)	0.86	11.82	$1.70 + j0.56$ (1.79)	0.95	0.44	10.74	1.08
1	0.00	$1.52 + j0.70$ (1.67)	$1.52 + j0.70$ (1.67)	0.91	10.02	$1.52 + j0.50$ (1.61)	0.94	0.20	9.66	0.36
2	0.00	$1.39 + j0.50$ (1.48)	$1.39 + j0.50$ (1.48)	0.94	8.88	$1.39 + j0.46$ (1.47)	0.95	0.04	8.82	0.06
3	0.00	$1.39 + j0.50$ (1.48)	$1.39 + j0.50$ (1.48)	0.94	8.88	$1.39 + j0.46$ (1.47)	0.95	0.04	8.82	0.06
4	0.00	$1.46 + j0.50$ (1.54)	$1.46 + j0.50$ (1.56)	0.93	9.36	$1.46 + j0.48$ (1.55)	0.94	0.02	9.30	0.06
5	0.00	$1.70 + j0.90$ (1.92)	$1.70 + j0.90$ (1.95)	0.87	11.70	$1.70 + j0.56$ (1.79)	0.95	0.34	10.74	0.96
6	0.50	$2.24 + j1.40$ (2.64)	$1.74 + j1.40$ (2.25)	0.77	14.63	$1.74 + j0.57$ (1.83)	0.95	0.83	11.90	2.73
7	1.20	$2.78 + j1.80$ (3.31)	$1.58 + j1.80$ (2.40)	0.66	16.80	$1.58 + j0.52$ (1.67)	0.95	1.28	11.69	5.11
8	2.20	$3.35 + j1.90$ (3.85)	$1.15 + j1.90$ (2.24)	0.51	16.80	$1.15 + j0.38$ (1.21)	0.95	1.52	9.08	7.73
9	3.00	$3.70 + j2.50$ (4.47)	$0.70 + j2.50$ (2.60)	0.27	20.80	$0.70 + j0.23$ (0.73)	0.95	2.27	5.84	14.96
10	3.50	$4.03 + j2.50$ (4.74)	$0.53 + j2.50$ (2.56)	0.21	21.76	$0.53 + j0.17$ (0.55)	0.96	2.33	4.68	17.09
11	4.00	$4.33 + j3.00$ (5.27)	$0.33 + j3.00$ (3.01)	0.11	27.09	$0.33 + j0.11$ (0.35)	0.95	2.89	3.15	23.94
12	3.50	$3.35 + j2.00$ (3.90)	$-0.15 + j2.00$ (2.01)	0.07	19.10	$-0.15 + j0.05$ (0.16)	0.94	1.95	−1.52	20.62
13	3.00	$3.16 + j1.80$ (3.64)	$0.16 + j1.80$ (1.81)	0.09	17.20	$0.16 + j0.05$ (0.17)	0.94	1.75	1.62	15.58
14	2.00	$2.78 + j1.50$ (3.16)	$0.78 + j1.50$ (1.68)	0.46	15.12	$0.78 + j0.26$ (0.82)	0.95	1.24	7.38	7.74
15	1.60	$2.55 + j1.30$ (2.86)	$0.95 + j1.30$ (1.61)	0.59	13.69	$0.95 + j0.31$ (1.01)	0.94	0.99	8.59	5.10
16	1.00	$2.15 + j1.20$ (2.46)	$1.15 + j1.20$ (1.66)	0.69	13.28	$1.15 + j0.38$ (1.21)	0.95	0.82	9.68	3.60
17	0.40	$3.14 + j1.80$ (3.62)	$2.74 + j1.80$ (3.30)	0.83	24.75	$2.74 + j0.90$ (2.91)	0.94	0.90	21.83	2.93
18	0.20	$3.81 + j2.50$ (4.56)	$3.61 + j2.50$ (4.34)	0.83	30.38	$3.61 + j1.19$ (3.83)	0.94	1.31	26.81	3.57
19	0.00	$4.06 + j3.00$ (5.05)	$4.06 + j3.00$ (5.05)	0.80	34.34	$4.06 + j1.33$ (4.24)	0.96	1.67	28.83	5.51
20	0.00	$3.47 + j2.00$ (4.01)	$3.47 + j2.00$ (4.00)	0.87	26.00	$3.47 + j1.14$ (3.70)	0.94	0.86	24.05	1.95
21	0.00	$2.68 + j1.50$ (3.07)	$2.68 + j1.50$ (3.07)	0.87	19.34	$2.68 + j0.88$ (2.84)	0.94	0.62	17.89	1.45
22	0.00	$2.15 + j1.20$ (2.46)	$2.15 + j1.20$ (2.48)	0.87	15.38	$2.15 + j0.71$ (2.25)	0.95	0.49	13.95	1.43
23	0.00	$1.70 + j1.00$ (1.97)	$1.70 + j1.00$ (1.97)	0.86	11.82	$1.70 + j0.56$ (1.79)	0.95	0.44	10.74	1.08
			Total Cost Before: 418.92	**After: 274.24**		**Savings: 144.67**				

The convex quadratic program is solved using an interior-point method owing to its robustness and computational efficiency for convex problems. A convergence tolerance of 10^{-6} is used, with a maximum of 10 iterations per control interval.

Active and reactive power at the PCC are computed using measured voltage and current signals. To mitigate measurement noise, a first-order digital low-pass filter with a cutoff frequency of 50 Hz is applied.

The weighting parameter $\lambda = 0.8$ is consistently used in both the optimization formulation and experimental implementation.

The optimization is executed at each control interval with a sampling step of $\Delta t = 2$ ms in a receding-horizon manner, where updated PCC measurements of load demand and PV generation are used at each step to compute fresh optimal set points. The supervisory layer operates at this 2 ms timescale, which is significantly slower than the inverter's inner current and voltage control loops, making it inherently insensitive to high-frequency measurement noise. Signal conditioning and anti-aliasing filtering are handled within the

TI C2000 DSP's built-in ADC interface and digital filtering stages. Sensing and actuation delays are effectively compensated by the fast inner control loops of the inverter, ensuring stable real-time operation. The convex nature of the optimization ensures smooth variation in set points, avoiding abrupt control actions.

4.3. Supervisory Control Flow

The control flow starts with sampling of PCC voltage and current. A programmable DC source is utilized to emulate PV generation. Resistive loads (e.g., lamps, heaters) are emulated using laboratory resistive elements, while inductive loads (e.g., fans, motors) are emulated using combinations of rheostats and inductors. The available laboratory load components are varied to match the characteristics of actual appliance loads.

The net active power demand, time-of-day tariffs and inverter rating are updated for the current interval in the control loop. This ensures that real-time data are utilized for decision making at each interval.

To solve the constraints, a convex quadratic program is formulated and solved using the interior-point method. This enables the calculation of optimal set point reference signals to the control loops of the inverter. The interior-point method is utilized because it guarantees convergence to a global optimum within the sampling period, thus ensuring a real-time implementation of the proposed algorithm. The solver is configured with a convergence tolerance of 10^{-6} and typically converges within approximately 10 iterations.

The computed set points are dispatched to the inverter. Parameters at the PCC are continuously monitored and provided to update the optimization in subsequent intervals. This control flow is formalized in Algorithm 1. The algorithm illustrates the practical implementation of the supervisory optimization framework on an embedded controller, ensuring that all constraints are satisfied and enabling real-time execution.

The final inverter set points are consistent with the optimal solution obtained from the quadratic program, and the two-stage structure represents an implementation mapping rather than a heuristic replacement.

Before hardware prototype development, simulations were carried out to verify the behavior of the proposed control algorithm. The PV generation profile used in the experiments—showing the MPPT voltage and current throughout the day—is illustrated in Figure 2. The simulated PCC and grid currents for typical daytime and nighttime periods are shown in Figures 3–6.

Figures 3 and 4 show the simulated midday operation, where high PV generation allows the inverter to export real power while the supervisory controller modulates reactive power to maintain the PCC power factor. The resulting grid current waveform reflects reduced reactive demand and effective utilization of the inverter's kVA capability.

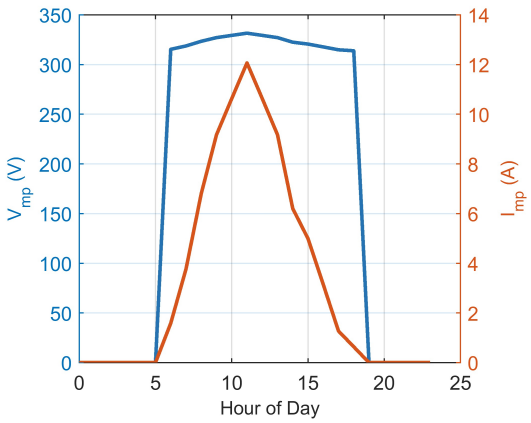


Figure 2. Voltage and current extracted by solar MPPT.

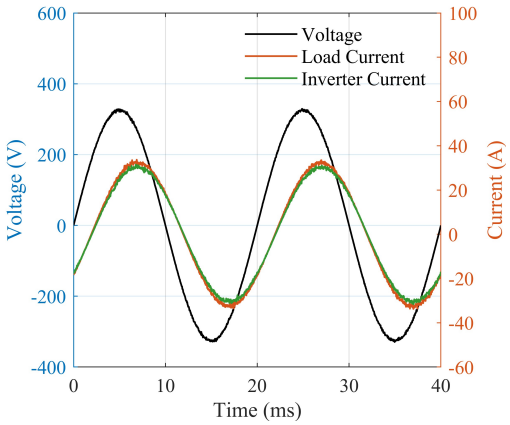


Figure 3. Simulated PCC voltage, inverter current, and load current during daytime operation.

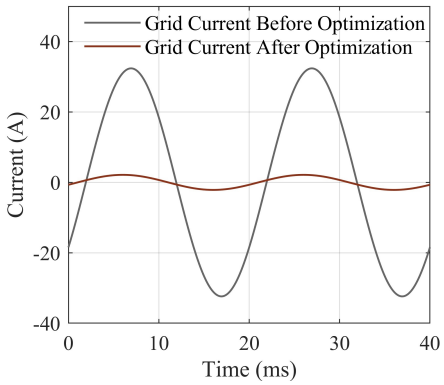


Figure 4. Simulated grid current during daytime operation.

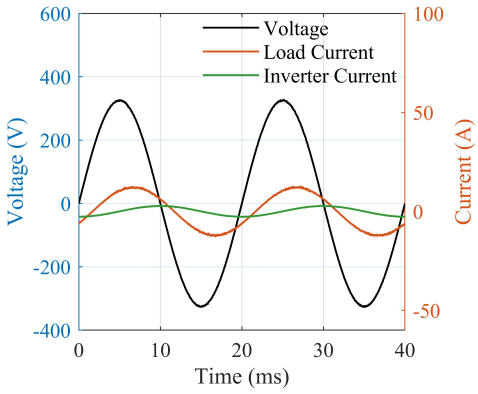


Figure 5. Simulated PCC voltage, inverter current, and load current during nighttime operation.

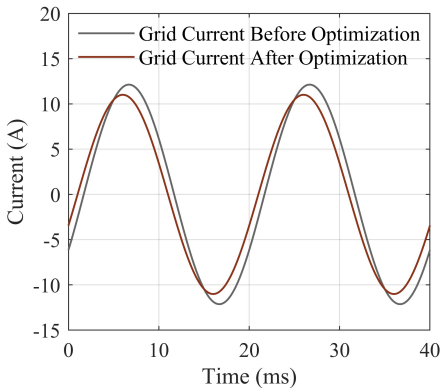


Figure 6. Simulated grid current during nighttime operation.

Figures 5 and 6 illustrate nighttime operation with zero PV generation. In this case, the grid supplies all real power, and the inverter provides controlled reactive compensation to ensure that the PCC power factor remains above the mandated threshold.

Algorithm 1 Supervisory optimization-based inverter control

Require: $P_{\text{PV}}(t), P_{\text{load}}(t), Q_{\text{load}}(t), S_{\text{inv}}, C_{\text{buy}}(t), C_{\text{sell}}(t)$
Ensure: $P^*_{\text{inv}}(t), Q^*_{\text{inv}}(t)$
Phase 1: Problem Formulation
Objective: Minimize $J = J_{\text{econ}} + \lambda J_{\text{grid}}$
where: $J_{\text{econ}} = C_{\text{buy}} P_{\text{import}} - C_{\text{sell}} P_{\text{export}}$
and: $J_{\text{grid}} = \left(Q_{\text{grid}} - k\, P_{\text{grid}}\right)^2$
Constraints:
$P^2_{\text{inv}} + Q^2_{\text{inv}} \leq S^2_{\text{inv}}$
$0 \leq P_{\text{inv}} \leq P_{\text{PV}}$
Phase 2: Constrained Optimization
Initialize: $P^0_{\text{inv}} \leftarrow \min(P_{\text{PV}}, P_{\text{load}})$, $Q^0_{\text{inv}} \leftarrow 0$, $\mu \leftarrow 1.0$, $\epsilon \leftarrow 10^{-6}$
for each control interval t **do**
Construct barrier function $B(\mathbf{x}(t))$
Compute Newton step: $\Delta\mathbf{x}(t) \leftarrow -\mathbf{H}^{-1}\nabla B(t)$
Update inverter set points:

$$\mathbf{x}^{(t)} \leftarrow \text{ProjectToFeasibleSet}(\mathbf{x}^{(t-1)} + \alpha\Delta\mathbf{x}(t))$$

if $\|\Delta\mathbf{x}(t)\| < \epsilon$ **then**
break
end if
Update barrier parameter: $\mu \leftarrow 0.5 \cdot \mu$
end for
Phase 3: Set point Dispatch
Obtain optimal solution $(P^*_{\text{inv}}, Q^*_{\text{inv}})$
Dispatch $(P^*_{\text{inv}}, Q^*_{\text{inv}})$ to inverter
return $(P^*_{\text{inv}}, Q^*_{\text{inv}})$

This pseudo-code demonstrates how the supervisory optimization is practically realized on the embedded controller. The interior-point iterations ensure that the constraints are respected, and the routine is completed within the sampling period, making it suitable for real-time deployment.

5. Results and Discussion

Table 3 summarizes the hourly operation of the PV–inverter system, including load, PV generation, grid injection before and after optimization, inverter reactive power contribution, cost, and savings. The complete dataset provided in Table 3 enables full reconstruction and verification of the system operation over the 24-h period. The proposed supervisory optimization maintains the power factor close to the desired threshold (approximately 0.94–0.96 under most operating conditions), with minor deviations under inverter capacity constraints.

It is observed that the power factor is maintained within the range of approximately 0.94–0.96. Minor deviations below 0.95 occur when the inverter operates near its apparent power limit, where strict PF enforcement would reduce economic benefit.

Figure 7 presents the hourly grid reactive power before and after optimization. It is evident that the optimization substantially reduces grid reactive power, particularly during midday and evening hours when PV generation is high. The percentage reduction is shown in Figure 8, where reductions exceeding 50% are achieved in most hours, confirming the effectiveness of the proposed strategy.

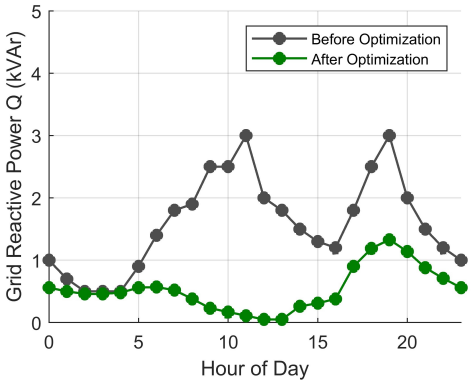


Figure 7. Hourly grid reactive power before vs. after optimization.

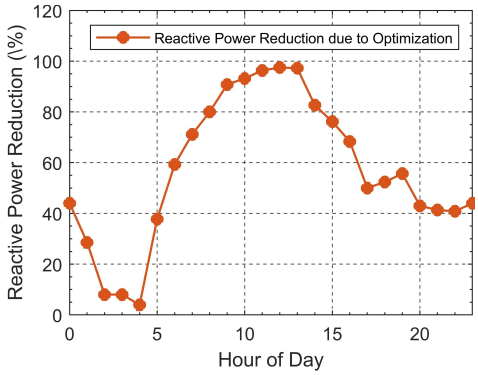


Figure 8. Percentage reduction in grid reactive power due to optimization.

Hourly inverter utilization is illustrated in Figures 9 and 10. During peak PV generation, the inverter operates near its rated capacity while retaining sufficient margin for reactive power support. The stacked bar plot demonstrates that high real power export and reactive compensation can be delivered simultaneously without exceeding the inverter's rated limits.

Economically, the optimization reduces daily electricity costs by scheduling PV export during high-tariff periods and minimizing reactive power drawn from the grid. Figure 11 depicts the hourly cost before and after optimization, highlighting peak savings during midday PV generation. Overall, the strategy achieves a cumulative cost reduction of Rs. 144.67 in the considered operating scenario, primarily driven by time-of-day tariff optimization.

The results demonstrate that the supervisory optimization strategy effectively balances technical and economic objectives. The primary economic benefit arises from time-of-day tariff optimization through strategic real power export. Reactive power control enhances inverter capacity utilization and improves power factor performance, indirectly supporting economic gains while reducing the grid reactive power burden.

An analysis of the hourly savings in Table 3 provides further insight into the individual contributions of each component. During nighttime hours (hours 0–5 and 19–23), where PV generation is zero, the inverter provides only reactive power compensation to reduce the apparent power drawn from the grid. The savings during these hours arise purely from reactive power management and amount to approximately Rs. 14.00, representing around 9.7% of total savings. During daytime hours (hours 6–18), both ToD-based real power export scheduling and reactive power compensation contribute to savings, amounting to approximately Rs. 130.70 (90.3% of total savings). The dominant contribution during the daytime arises from the strategic export of real power during high-tariff periods, while the management of reactive power provides additional benefit through improved inverter utilization.

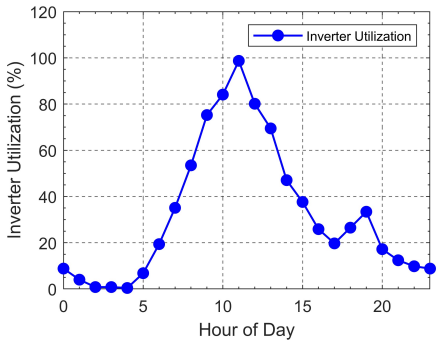


Figure 9. Hourly inverter utilization (%).

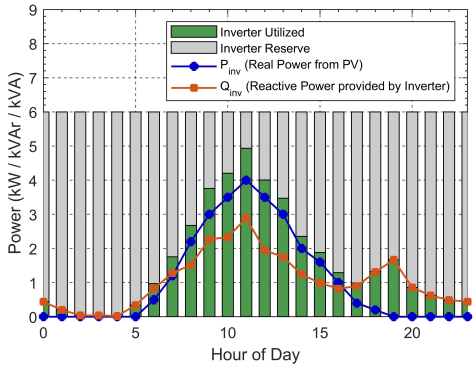


Figure 10. Inverter's apparent power utilization and PV availability.

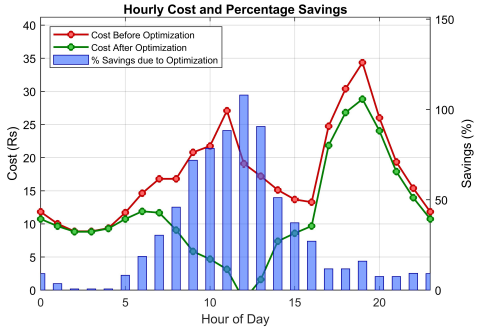


Figure 11. Hourly grid cost before and after optimization, showing savings through strategic PV export and reactive power compensation.

To assess measurement reliability and repeatability, multiple experimental runs were conducted under identical operating conditions. The variation in key performance indicators, including power factor and cost savings, was observed to be within approximately ±2%, indicating consistent system performance.

The measurements are obtained using calibrated voltage and current sensors with appropriate signal conditioning and filtering, ensuring reliable data acquisition.

The results demonstrated consistent behavior across varying operating conditions, including changes in load demand, PV generation, and tariff levels. The observed improvements in power factor, reduction in grid reactive power, and cost savings remained consistent across repeated trials, confirming the reliability of the proposed control strategy. These results provide quantitative validation of the proposed method and confirm its effectiveness under practical operating conditions.

In comparison to conventional Volt/VAR droop control, which regulates reactive power solely on the local voltage using predefined static characteristics, the proposed optimization-based approach provides a more flexible and adaptive control framework.

Conventional volt/VAR droop control operates on the basis of predefined voltage–reactive power characteristics and does not explicitly consider economic objectives or optimal allocation of inverter capacity. In contrast, the proposed optimization-based approach dynamically coordinates real and reactive power by incorporating time-of-day tariffs, inverter constraints, and power factor requirements. The results demonstrate that the proposed method achieves a significant reduction in grid reactive power (exceeding 50% in several operating intervals) while maintaining the power factor close to the desired range (approximately 0.94–0.96). This comparison highlights the advantage of the proposed method in achieving coordinated techno-economic operation. While a direct experimental comparison with droop control is not included, the qualitative analysis highlights the inherent limitations of droop-based methods and the advantages of the proposed optimization-based approach.

6. Conclusions and Future Work

The proposed supervisory optimization strategy for residential PV inverters has been implemented and validated on a real-time laboratory prototype. The results demonstrate that the controller maintains the power factor close to the desired regulatory threshold, improves inverter utilization, and reduces electricity cost through coordinated management of real and reactive power. The proposed approach enables a practical realization of a multi-objective optimization framework in real time without violating inverter operating limits.

The proposed method operates in a measurement-driven manner and adapts to real-time variations in load and PV generation. Future work will focus on incorporating uncertainty-aware and predictive optimization techniques to further enhance performance under stochastic operating conditions. The present study focuses on a single-inverter household-level implementation. While the proposed method is inherently scalable, feeder-level impacts such as voltage profile improvement and loss reduction are not explicitly evaluated and will be considered in future work.The proposed supervisory control strategy can be extended to multi-inverter systems or microgrid environments, where coordination between multiple distributed resources becomes important. Future work will focus on distributed optimization approaches for scalable implementation, as well as incorporating dynamic tariffs, stochastic PV generation, and load forecasting. The inclusion of energy storage systems can further enhance system flexibility and improve performance under highly variable operating conditions.

Author Contributions: A.A. conceptualized the study, performed the experiments, collected and analyzed the data, and drafted the manuscript. S.M. supervised the research work, reviewed and edited the manuscript, and contributed to the interpretation of results. A.M. and S.P. provided guidance on work methodology and experimental results. All authors have read and agreed to the published version of the manuscript.

Funding: This research received no external funding.

Data Availability Statement: Data is contained within the article: The original contributions presented in this study are included in the article

Acknowledgments: The authors gratefully acknowledge PSG College of Technology for providing the research facilities and institutional support necessary to carry out this work. The authors also acknowledge the Special Machines Laboratory, the Embedded and Real-Time Systems Laboratory, and the Centre for Welding Technology (Tech-2) in the Department of Electrical and Electronics Engineering, PSG College of Technology, for their support in the development and experimental validation of the hardware prototype.

Conflicts of Interest: The authors declare no conflicts of interest.

Abbreviations

The following abbreviations are used in this manuscript:

PF	Power Factor
ToD	Time-of-Day
PV	Photovoltaic
CQP	Convex Quadratic Programming
PCC	Point of Common Coupling
P	Real Power
Q	Reactive Power

References

1. Zheng, Y.; Catun, S.; Manaz, M.A.M.; Lu, C.N. Unlocking Virtual Feeder Hosting Capability for Renewable Integrations via P2P Ancillary Service Trading. *IEEE Trans. Ind. Appl.* **2025**, *61*, 8100–8110. [CrossRef]
2. Gaurav, S.; Pugliese, S.; Langwasser, M.; Kumar, C.; Liserre, M. Power Control in Andronov-Hopf Virtual Oscillator Converters for ST-Based LV Distribution Systems. *IEEE Trans. Ind. Electron.* **2025**, *72*, 9239–9249. [CrossRef]
3. Guo, Z.; Qu, X.; Liu, J.; Li, Y.; Tse, C.K. Unilateral Compensation for Compact and Lightweight IPT Converters with Near Unity Power Factor and Load-Independent Constant Output. *IEEE Trans. Power Electron.* **2025**, *40*, 10189–10197. [CrossRef]
4. Karamdel, S.; Liang, X.; Faried, S.O. A Novel Stochastic Volt/VAR/Pressure Optimization-Based Conservation Voltage Reduction Technique in Integrated Electricity and Natural Gas Systems with PV Smart Inverters. *IEEE Trans. Ind. Appl.* **2025**, *61*, 2271–2286. [CrossRef]
5. Inaolaji, A.; Savasci, A.; Paudyal, S. Distribution Grid Optimal Power Flow in Unbalanced Multiphase Networks With Volt-VAr and Volt-Watt Droop Settings of Smart Inverters. *IEEE Trans. Ind. Appl.* **2022**, *58*, 5832–5843. [CrossRef]
6. Das, A.; Batzelis, E.I.; Anand, S.; Sahoo, S.R. Network-Agnostic Adaptive PQ Adjustment Control for Grid Voltage Regulation in PV Systems. *IEEE Trans. Ind. Appl.* **2022**, *58*, 5792–5804. [CrossRef]
7. Roncero-Clemente, C.; Husev, O.; Matiushkin, O.; Vinnikov, D.; Blaabjerg, F. Reactive Power Injection Capability of Buck–Boost Inverter with Unfolding Circuit. *IEEE Trans. Power Electron.* **2022**, *37*, 11876–11886. [CrossRef]
8. Satsangi, S.; Kumbhar, G.B. Energy Savings Estimation of a Distribution System in Presence of Intelligent Volt-VAr Control Based on IEEE Std. 1547-2018. *CSEE J. Power Energy Syst.* **2022**, *8*, 1477–1486. [CrossRef]
9. Dutta, A.; Ganguly, S.; Kumar, C. MPC-Based Coordinated Voltage Control in Active Distribution Networks Incorporating CVR and DR. *IEEE Trans. Ind. Appl.* **2022**, *58*, 4309–4318. [CrossRef]
10. Vijayan, V.; Mohapatra, A.; Singh, S.N. A Topology Assisted Optimal CVR Strategy for Unbalanced EDNs Having Spatio-Temporal Loads. *IEEE Trans. Ind. Appl.* **2022**, *58*, 3313–3323. [CrossRef]
11. Das, A.; Gupta, Y.; Anand, S.; Sahoo, S.R. Temperature Droop-Based Dynamic Reactive Power Sharing Technique to Improve the Lifetime of Power Electronic Converter. *IEEE Trans. Power Electron.* **2022**, *37*, 5245–5255. [CrossRef]
12. Chen, J. A Novel Modulation Method for LLC Converter-Based Semi-Single-Stage Isolated Inverter With Hybrid Sliding Mode Control. *IEEE Trans. Power Electron.* **2025**, *40*, 704–715. [CrossRef]
13. Glover, D.; Dubey, A. Learning Volt-VAR Droop Curves to Optimally Coordinate Photovoltaic (PV) Smart Inverters. *IEEE Trans. Ind. Appl.* **2025**, *61*, 859–871. [CrossRef]
14. Deng, X. Virtual Vector Modulation and Capacitor Voltage Control for Coupled Eight-Switch Three-Phase Three-Level Inverter With Full Lagging Reactive Power Flow Capability. *IEEE Trans. Ind. Electron.* **2025**, *72*, 16–26. [CrossRef]
15. Li, H.; Tan, L.; Xu, H.; Wu, Z.; Huang, X. A Wide-Range Global Optimal Control Strategy for Wireless Charging Systems in Electric Vehicles. *IEEE Trans. Power Electron.* **2024**, *39*, 16864–16876. [CrossRef]
16. Sahoo, B.; Samantaray, S.R.; Rout, P.K. Adaptive Control Scheme for Hybrid Microgrid Resynchronization with Virtual Synchronous Generator and Active Detection Technique. *IEEE Trans. Ind. Appl.* **2024**, *60*, 7599–7612. [CrossRef]
17. Zhang, K.; Wang, L.; Lv, Y.; Yang, C.; Wong, M.C. Analysis and Control of the Injected Type-Adaptive Impedance (IT-AI) Inverter for Low-Capacity Requirement. *IEEE Trans. Ind. Electron.* **2024**, *71*, 13513–13523. [CrossRef]
18. Poudel, S. A Two-Stage Approach for PV Inverter Engagement in Power Factor Correction and Voltage Regulation. *IEEE Trans. Ind. Appl.* **2025**, *61*, 2527–2537. [CrossRef]
19. Boopathi, R.; Indragandhi, V. Enhancement of power quality in grid-connected systems using a predictive direct power controlled based PV-interfaced with multilevel inverter shunt active power filter. *Sci. Rep.* **2025**, *15*, 7967. [CrossRef] [PubMed]
20. Ahn, B. An Overview of Cyber-Resilient Smart Inverters Based on Practical Attack Models. *IEEE Trans. Power Electron.* **2024**, *39*, 4657–4673. [CrossRef]

21. Altaf, M.W. Control and Protection Scheme for DC-Link of Solar PV Based Microgrid. *IEEE Trans. Ind. Appl.* **2024**, *60*, 2706–2715. [CrossRef]
22. He, W.; Qiu, D.; Zhang, B.; Chen, Y.; Xie, F.; Xiao, W. Extending the Operation Range of Electric Spring With Dual Inverters. *IEEE Trans. Power Electron.* **2024**, *39*, 3544–3557. [CrossRef]
23. Kumar, K.; Satsangi, S.; Kumbhar, G.B. Extension of Distribution Transformer Life in the Presence of Smart Inverter-based Distributed Solar Photovoltaic Systems. *CSEE J. Power Energy Syst.* **2024**, *10*, 88–95. [CrossRef]
24. Patekar, R.S.; Pal, D.; Panigrahi, B.K. Event-Triggered Hybrid Anti-Islanding Protection Scheme Based on Q-Axis Disturbance Injection. *IEEE Trans. Ind. Electron.* **2024**, *71*, 5787–5796. [CrossRef]
25. Naderi, E.; Mirzaei, L.; Pourakbari-Kasmaei, M.; Cerna, F.V.; Lehtonen, M. Optimization of active power dispatch considering unified power flow controller: Application of evolutionary algorithms in a fuzzy framework. *Evol. Intell.* **2024**, *17*, 1357–1387. [CrossRef]
26. Naderi, E.; Mirzaei, L.; Trimble, J.P.; Cantrell, D.A. Multi-Objective Optimal Power Flow Incorporating Flexible Alternating Current Transmission Systems: Application of a Wavelet-Oriented Evolutionary Algorithm. *Electr. Power Compon. Syst.* **2024**, *52*, 766–795. [CrossRef]

Disclaimer/Publisher's Note: The statements, opinions and data contained in all publications are solely those of the individual author(s) and contributor(s) and not of MDPI and/or the editor(s). MDPI and/or the editor(s) disclaim responsibility for any injury to people or property resulting from any ideas, methods, instructions or products referred to in the content.